Causes of crack formation during plastic deformation of corrosion-resistant austenitic-martensitic steel (case study of 07Kh16N6 steel)

S. G. Ivanov, *Dr. Eng., Leading Researcher [1,2], Leading Researcher of Hubei Digital Textile Equipment Key Laboratory [3], e-mail: serg225582@yandex.ru;*
M. A. Guryev, *Cand. Eng., Associate Prof., Dept. of Mechanical Engineering Technology [1], Technical Director [4], e-mail: gurievma@mail.ru*
V. B. Deev*, *Dr. Eng., Prof., Prof. of Digital Textile Equipment Key Laboratory [3], Head of the Dept. of Equipment and Technologies of the Welding [5], Chief Researcher [6], e-mail: deev.vb@mail.ru;*
M. N. Zenin, *Postgraduate Student, Junior Researcher, Engineer of the Department of Modern Special Materials [1], e-mail: mikhail.zenin.96@mail.ru*

[1] *Polzunov Altai State Technical University (Barnaul, Russia)*
[2] *The Advanced Textile Technology Innovation Center (Jianhu Laboratory) (Shaoxing, China)*
[3] *Wuhan Textile University (Wuhan, China)*
[4] *Zhejiang Briliant Refrigeration Equipment Co., Ltd. (Xingchang, China)*
[5] *Moscow Polytechnic University (Moscow, Russia)*
[6] *Vladimir State University named after Alexander and Nikolay Stoletovs (Vladimir, Russia)*

**Corresponding author: deev.vb@mail.ru*

High-chromium, low-nickel corrosion-resistant steels of the austenitic-martensitic class exhibit excellent corrosion resistance along with reasonably good mechanical strength, making them promising for various applications in mechanical engineering and building construction. Upon plastic deformation, their strength characteristics can further increase. However, the widespread industrial application of these steels is constrained by the complexity of their plastic forming processes (e.g., stamping, upsetting), due to a high propensity for cracking, which results in defects in the final products. This study investigates the causes of cracking in austenitic-martensitic corrosion-resistant steels during plastic deformation, using high-chromium, low-nickel steel grade 07Kh16N6 as a representative material. Metallographic analysis reveals that the primary cause of crack formation during plastic deformation is the formation of deformation-induced martensite, which is associated with a negative volume change. This local volume contraction leads to the development of tensile stresses at sites of martensitic transformation. It is reasonable to assume that when large volumes of deformation-induced martensite form rapidly, the resulting tensile stresses may exceed the material's strength, thereby initiating cracking. Moreover, the generated tensile stresses can also promote the formation of so-called athermal martensite, which is accompanied by a slight volume expansion and, thus, a partial compensation of the tensile stresses. However, at high deformation rates, the formation of athermal martensite tends to lag behind the transformation-induced martensitic process, exacerbating the tendency for crack initiation and propagation. This hypothesis is indirectly supported by other researchers, who have also identified optimal strain rates ($6.67 \cdot 10^{-4}$ s^{-1}) and maximum allowable single-pass reduction ratio (no more than 19–22 %). In cases where higher reduction ratios are required, a multi-pass deformation strategy with intermediate recrystallization annealing is recommended to eliminate the martensitic phase and reduce cracking risk.
Key words: deformation-induced martensite, austenitic-martensitic steel, cracking, plastic deformation.
DOI: 10.17580/cisisr.2025.02.05

Introduction

Ensuring the operational integrity, reliability, and service life of various types of special-purpose equipment operating under intensive mechanical loads combined with corrosive environmental exposure requires a comprehensive approach to the selection of structural materials and the targeted control of their property formation processes. The conditions of steel melting and casting solidification [1–3], as well as the thermomechanical processing of workpieces [4, 5], along with many other factors, significantly influence the formation of the desired microstructure and the operational characteristics of the final products.

A promising group of materials is duplex corrosion-resistant stainless steels of the austenitic-martensitic type, such as steel grade 07Kh16N6 (Russia) [6]. These steels exhibit a highly favorable combination of mechanical properties, corrosion resistance, and good weldability. However, the manufacturing of machine components and structural elements from this steel presents a number of technological challenges, the most critical of which is the material's tendency to undergo strain-induced hardening during plastic deformation processes such as stamping and forging. This is due to the presence of metastable austenite, which is prone to martensitic transformation under deformation. International equivalents of steel 07Kh16N6 include SUS 301 (Japan), AISI 301 (USA), and BS301S21 (UK).

Austenitic-martensitic (transitional) corrosion-resistant steels combine the ductility typical of austenitic grades with the strength of martensitic steels. These are chromium-nickel alloys such as 09Kh15N9Yu, 08Kh17N8Yu, 07Kh16N6, and others. Their chemical composition is optimized so that the start temperature of the athermal martensitic transformation (Ms) lies close to room temperature, while the start of the strain-induced martensitic transformation (Md) is above room temperature. Athermal martensite is usually understood to mean martensite that is formed as a result of a sharp rearrangement of the crystal lattice during significant supercooling of austenite (the so-called quenching martensite, since it is formed most often during the quenching of steels). The term "athermal martensite" is used in this paper to differentiate between types of martensite, since the paper also discusses the formation of "deformation martensite", which is formed under the action of and as a result of deformation. Following quenching, these steels typically possess a metastable austenitic structure capable of undergoing $\gamma \rightarrow \alpha$'-martensitic transformation under cold treatment or plastic deformation below Md. In addition to austenite, the microstructure may contain small amounts of martensite (typically 5–10 %) and δ-ferrite, which is also usually limited to no more than 10 %. The δ-ferrite content must be controlled to avoid embrittlement and degradation of mechanical performance. The properties of these steels are largely determined by the ratio between austenite and martensite in the microstructure. This phase balance, as well as the stability of the retained austenite, is governed by alloying elements, thermal treatment, and the level of plastic deformation.

Upon slow cooling, chromium-nickel corrosion-resistant transitional steels such as 07Kh16N6 typically form a structure comprising austenite (γ), ferrite (α), and $M_{23}C_6$ carbides. To obtain a fully austenitic microstructure with enhanced corrosion resistance, these steels are reheated to 1100–1150 °C (to dissolve carbides) followed by water quenching or air cooling. The resulting austenite phase is relatively unstable and tends to transform into deformation-induced martensite under mechanical strain [7–14].

If austenitic stainless steels are held at intermediate temperatures (ranging from 500 °C to 950 °C) during cooling, this leads to carbon diffusion and the precipitation of carbides (this operation is also called aging). This, in turn, results in material strengthening but also increases the susceptibility to intergranular corrosion in aggressive environments due to chromium depletion along grain boundaries. The primary carbide in steel grade 07Kh16N6 is the $M_{23}C_6$-type carbide, though other types such as M_7C_3, M_6C, and MC may also form. The exact composition of the carbides may vary depending on the alloy's chemistry. The precipitation of $Cr_{23}C_6$ occurs predominantly at grain boundaries, leading to the formation of chromium-depleted zones near these boundaries. For this reason, austenitic steels to avoid aging are rapidly cooled from the austenitization temperature to avoid carbide formation.

Alternatively, carbides can be dissolved by solution heat treatment followed by rapid quenching. Therefore, carbide formation poses a serious issue for austenitic stainless steels.

In metastable duplex ferritic–martensitic stainless steels, austenite can transform into two distinct types of martensite: hexagonal close-packed (HCP) martensite, referred to as ε-martensite or "strain-induced martensite" due to its formation during plastic deformation, and body-centered cubic (BCC) martensite, known as α-martensite. The formation of martensitic phases causes a change in volume relative to the original austenite: α-martensite leads to a volume expansion of 1–4 %, whereas ε-martensite leads to a volume contraction. It has been reported [15] that α-martensite nucleates within dislocation clusters, whereas ε-martensite nucleates at stacking faults. It is hypothesized that the initial α-martensite nucleus is coherent with the parent austenite. As α-martensite plates grow, they likely become semi-coherent or incoherent. In contrast, ε-martensite is believed to remain coherent with the austenite matrix.

In addition to the factors shared with spontaneous martensitic transformation, there are specific parameters that must be considered for deformation-induced martensitic transformation in metastable stainless steels. The concept of deformation-induced transformation implies that martensite can form even when the temperature is above Ms (the martensite start temperature). Deformation facilitates the initiation of the transformation, and deformation-induced martensitic transformation can be categorized into two types. The first type involves stress-assisted martensitic transformation, where applied stress promotes the onset of transformation even above the Ms temperature. The second type is strain-induced martensitic transformation, in which dislocations formed during plastic deformation serve as nucleation sites for martensite. Stress-assisted transformation typically occurs at low temperatures (but above Ms), while strain-induced transformation occurs at higher temperatures, including room temperature [16]. Thus, temperature plays a critical role in deformation-induced transformation, as it does in spontaneous transformation. As shown in **Fig. 1** [17], the transformation is enhanced at lower temperatures.

The aim of this study was a comprehensive analysis of crack formation processes during plastic deformation of corrosion-resistant austenitic-martensitic steel grade 07Kh16N6.

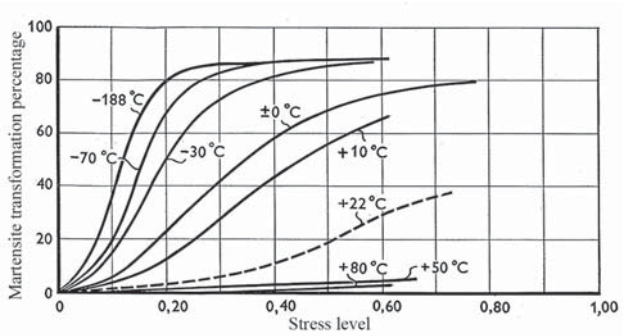

Fig. 1. Acceleration of martensitic transformation in metastable stainless steels caused by de-formation at low temperatures [17]

Methods

For the purposes of this study, the samples were extracted from the final part after the completion of cold plastic deformation by stamping. As a result of the stamping process, through-thickness cracks were observed in areas of the component subjected to substantial plastic deformation exceeding 35 %. The deformation rate was maintained at $5 \cdot 10^{-4}$ s^{-1}, and the total strain was accumulated over six deformation cycles, with each cycle imparting approximately 6 % strain. Intermediate heat treatment between deformation cycles was not performed.

Since the transformation occurs at temperatures above the martensite start temperature (Ms), the stability of these steels is assessed using alternative temperature-related parameters. One such parameter is the deformation-induced martensite start temperature (Md), which denotes the upper limit for martensitic transformation under mechanical deformation. Above the Md temperature, deformation-induced martensite typically does not form. However, direct measurement of Md is challenging; therefore, an alternative parameter, Md30, has been introduced [17]. Md30 is defined as the temperature at which 50 % of martensite forms under 30% true strain. This temperature is considered a reliable indicator of austenite stability in stainless steels susceptible to strain-induced martensitic transformation. Stability is determined by chemical composition, which is expressed in Angel's empirical formula:

$$Md30 = 413 - 462(C + N) - 9.2Si - 8.1Mn - 13.7Cr - 9.5э - 18.5Mo, \quad (1)$$

where C, N, Si, Mn, Cr, Ni, Mo are the corresponding chemical elements, taken in mass percentages.

The literature also contains a similar formula for determining the Md30 temperature, proposed by Nohara et al. [18] by refining Angel's formula:

$$Md30 = 551 - 462(C + N) - 9.2Si - 8.1Mn - 13.7Cr - 29(Ni + Cu) - 18{,}5Mo - 68Nb, \quad (2)$$

The above equations show that a greater amount of alloying additives increases the stability of austenite.

Martensite is harder and stronger than austenite. Consequently, metastable stainless steels exhibit high strain hardening capability during deformation due to both the increased dislocation density and the additional strengthening induced by martensitic transformation. Annealed austenitic stainless steels typically possess elongation values of about 50 %; however, metastable stainless steels demonstrate enhanced ductility owing to the TRIP effect (Transformation-Induced Plasticity), which is activated by the strain-induced martensitic transformation [7]. The TRIP effect is associated with high work-hardening rates, which suppress necking and thus extend the regime of uniform plastic deformation.

Other critical parameters that influence strain-induced martensitic transformation include the deformation mode and strain rate. Patel [19] found that uniaxial tension is more conducive to martensite formation than either uniaxial or multiaxial compression. Low strain rates promote martensitic transformation, whereas high strain rates generate adiabatic heating, which inhibits the transformation. At high strain rates, the onset temperature of deformation-induced transformation increases by approximately 90–95 °C [20–22].

The mathematical sigmoidal function, established in the range of true strains from 0.05 to εu (strain corresponding to the maximum load) in [22], is defined as follows:

$$\log\sigma = A + (B - A)/(1 + \exp(\log\varepsilon - \alpha)(\beta)^{-1})^{-1}, \quad (3)$$

where: σ – true stress in MPa; A – maximum logarithm of true stress ($\log\sigma_{max}$) when the sigmoidal function flattens out after the martensitic transformation reaches saturation (value of 3.18 at 30 °C and strain rate $6.67 \cdot 10^{-4}$ s^{-1}); B – minimum logarithm of true stress ($\log\sigma_{min}$) before any martensitic transformation (value of 2.73 at 30 °C and strain rate $6.67 \cdot 10^{-4}$ s^{-1}); ε – true strain; α – maximum sensitivity to deformation, which corresponds to the logarithm of true deformation at which the maximum slope of the log – log plot of true stress-true strain curve is achieved (value of –0.73 at 30 °C, ε = 0.19, and strain rate $6.67 \cdot 10^{-4}$ s^{-1}); β – a constant that indicates the degree of change in the logarithmic-logarithmic curves of true stress and true strain. The numerical value is determined by the formula $\beta = (A - B)(4 \cdot n_i)$-1. (Value of 0.11 at 30 °C, ε = 0.19, and strain rate $6.67 \cdot 10^{-4}$ s^{-1}).

In [23], the following conditions were proposed for obtaining a material that retains good plasticity and resistance to bending:

– the chemical composition should be balanced in such a way as to obtain Md30 in the range of 28–30 °C;

– during annealing, it is recommended to use an inert gas or nitrogen atmosphere to prevent changes in the chemical composition on the surface due to decarburization and denitriding;

– the recrystallization annealing temperature is at least 1060 °C;

– the final reduction during cold rolling should be between 19 % and 22 %.

Strengthening during cold deformation is associated with strain hardening and the occurrence of a martensitic transformation. The less stable the austenite, the more intensively it transforms into martensite (strain-induced martensite) during cold deformation.

The γ → α′ transformation can also occur upon heating within a temperature range where the most intense precipitation of carbides from austenite takes place (typically 700–750 °C). In this temperature interval, austenite becomes depleted in carbon and in alloying elements that are incorporated into the precipitated carbides, leading to an increase in the martensite start temperature (Ms), a reduction in austenite stability, and an increase in the amount of martensite formed. For example, during the precipitation of chromium carbides $(Fe,Cr)_{23}C_6$, the austenite becomes depleted in both carbon and chromium.

Specimens cut using an electrical discharge machine were mounted in Bakelit-B thermosetting resin using a MetaPress mounting press. Grinding and polishing were carried out on a DIGIPREP automatic grinder-polisher using diamond discs. Final polishing was performed using MET-Mambo cloths and polycrystalline diamond suspensions. The final preparation step involved electrolytic polishing using a Pulitrol unit with an electrolyte composed of 600 ml ethanol,

Table 1. Results of the chemical composition analysis of steel

Sample, steel	Element content, mass. %						
	C	Si	Mn	Cr	Ni	Ti	Al
Sample	0.056 ± 0.0036	0.178 ± 0.0012	0.426 ± 0.0044	17.101 ± 0.0561	6.087 ± 0.012	0.006 ± 0.00058	0.078 ± 0.005
07Kh16N6[1]	0.05–0.09	≤0.80	≤0.80	15.50–17.50	5.00–8.00	–	–
	W	Mo	Nb	V	S	P	
Sample	0.017 ± 0.00100	0.086 ± 0.00058	0.002	0.004 ± 0.00058	0.0160 ± 0.0005	0.0191 ± 0.0009	
07Kh16N6[1]	–	–	–	–	≤0.020	≤0.035	

[1] GOST 5632-2014 "Corrosion-resistant, heat-resistant, and high-temperature alloys and stainless steels. Grades"

240 ml butoxyethanol, and 60 ml perchloric acid, at an operating voltage of 53 V and at room temperature. Etching of the prepared metallographic specimens was performed using a mixture of concentrated nitric and hydrochloric acids in a 3:1 ratio (aqua regia). The chemical composition of the steel was determined by optical emission spectroscopy using a GNR Solaris CCD Pro spectrometer.

Results and Discussion

The steel investigated in the present study, in terms of its elemental composition (**Table 1**), corresponds to grade 07Kh16N6 according to GOST 5632-2014 "Corrosion-resistant, heat-resistant, and high-temperature alloys and stainless steels. Grades".

According to the calculations, the temperature of the onset of strain-induced martensite formation (Md_{30}), as determined using the expression proposed by Nohara et al. [18], for the investigated steel is 103 °C. In contrast, the temperature calculated using Angel's formula [17] is 88 °C.

The steel microstructure was examined on both transverse and longitudinal metallographic sections (**Fig. 2** and **Fig. 3**). As can be seen in these figures, the structural-phase state of steel grade 07Kh16N after complete deformation in crack-free components is represented predominantly by martensite. Due to the characteristic deformation texture, the martensite is primarily ε-martensite formed as a result of plastic deformation. The microstructure and structural-phase state of a similar component made of steel grade 07Kh16N6, subjected to rapid and complete deformation with crack formation, are shown in **Fig. 4** and **Fig. 5**. Regions exhibiting the coexistence of classical (athermal) α-martensite and deformation-induced ε-martensite are presented in **Fig. 6**.

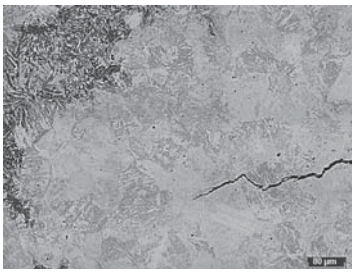

Fig. 4. Microstructure of the specimen near the crack initiation site after 60 % total deformation (strain rate $5 \cdot 10^{-4}$ s^{-1})

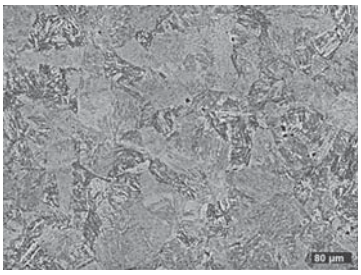

Fig. 2. Microstructure of 07Kh16N6 steel after 60 % total deformation (strain rate $5 \cdot 10^{-4}$ s^{-1}) in a crack-free region

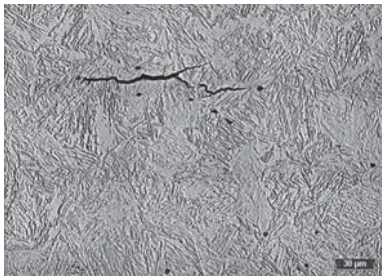

Fig. 5. Microstructure of 07Kh16N6 steel containing a microcrack after 60 % total deformation (strain rate $5 \cdot 10^{-4}$ s^{-1})

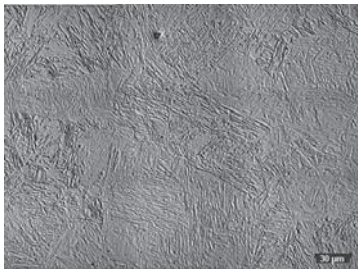

Fig. 3. Structural-phase state of 07Kh16N6 steel after 60 % total deformation (strain rate $5 \cdot 10^{-4}$ s^{-1}), in a crack-free region

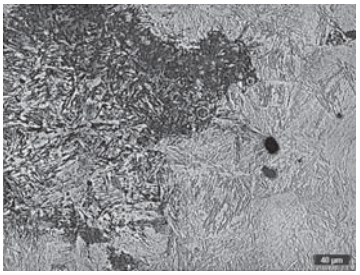

Fig. 6. α-martensite (left side of microstructure image) and ε-martensite (right side of image) in 07Kh16N6 steel after 60 % plastic deformation (strain rate $5 \cdot 10^{-4}$ s^{-1}).

As can be seen from the microstructural photographs presented in Fig. 4–6, the region of microcrack initiation exhibits the presence of α-martensite formed via an athermal mechanism. It is important to note that the cracks and their nuclei are located within the matrix of ε-martensite, which is formed through a deformation-induced mechanism. To differentiate between α- and ε-martensite, a color etching technique recommended in [24–28] was employed, whereby α-martensite stained brown, blue, and gray, whereas ε-martensite remained uncolored.

Based on the spatial distribution of the cracks, the most probable cause of their formation is a negative volumetric change, attributed on one hand to the volume contraction occurring during the formation of deformation-induced martensite, which simultaneously enhances the material's strength while reducing its ductility [29]. This negative volumetric change is partially compensated by the formation of -martensite via the athermal transformation of austenite, which involves a volume expansion. However, the fraction of athermal martensite formed during steel deformation depends on the strain rate and decreases at relatively low deformation rates, thereby insufficiently compensating for the negative volumetric change associated with deformation-induced martensite due to the comparatively smaller volume of the forming athermal martensite.

According to the analysis of the prior austenite grain size (**Fig. 7** and **Fig. 8**, **Table 2**), performed in accordance with GOST 5639-82 excluding boundary grains, the average grain size number was 6.5, corresponding to an average grain diameter of 27.57 μm. The conducted analysis of the distribution and ratio of athermal and deformation-induced martensite is shown in **Fig. 9**, while the grain size distribution of athermal and deformation-induced martensite individually is presented in **Fig. 10**. As evidenced by these results, deformation-induced martensite consists of coarser grains, indicating that its formation precedes that of athermal martensite [30–34]. Considering that the formation of deformation-induced martensite involves a slight volume contraction (≈1 %), this in turn partially reduces the stress level and may trigger (and indeed triggers) the athermal decomposition of austenite due to the decreased stability of the supercooled austenite [29–32]. The athermal transformation of austenite leads to volume expansion and thus an increase in internal stresses, which consequently causes grain refinement of the athermal martensite [33–38].

Taking into account the results of phase analysis of the distribution of athermal and deformation-induced martensite, the results of which are presented in Fig. 9, where

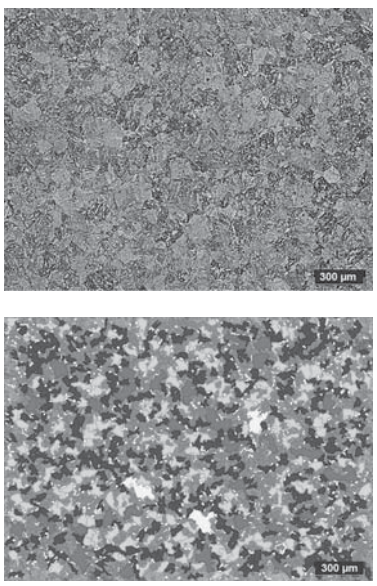

a

b

Fig. 7. Average grain size: (*a*) microstructure photograph; (*b*) analysis results

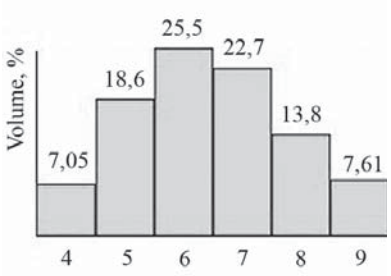

a

№	Color	Grade	Volume, %	Quantity, pcs
1		4	7,05	33
2		5	18,6	163
3		6	25,5	448
4		7	22,7	776
5		8	13,8	931
6		9	7,61	1013
Number of object				4536
Mean value				6,52

b

Fig. 8. Histogram of grain size distribution by scores (*a*) and color coding of grain scores (*b*) according to Fig. 6*b*

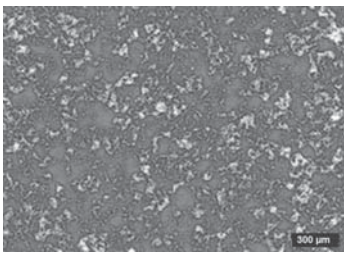

a

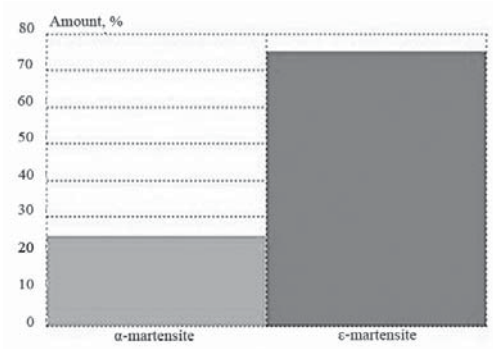

b

Fig. 9. Distribution of athermal («martensite A») and deformation («martensite D») marten-site across the polished section plane: (*a*) spatial distribution; (*b*) volumetric ratio between athermal and deformation martensite

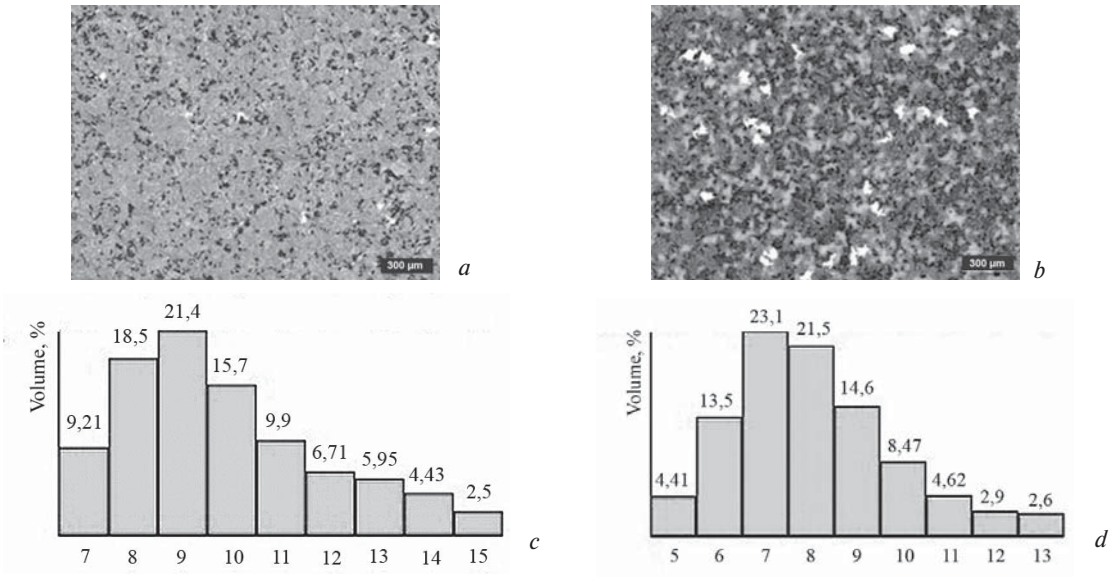

Fig. 10. Grain size in (*a*) athermal α-martensite and (*b*) deformation ε-martensite; (*c*) and (*d*) corresponding distributions of grain scores in athermal and deformation martensite, respectively

the distribution of athermal and deformation martensite is shown (Fig. 9a), and their volumetric fractions are determined (Fig. 9b), the ratio of deformation martensite to athermal martensite in the investigated specimen is 0.75:0.25, respectively.

The implementation of research findings on metastable austenitic-martensitic corrosion-resistant steels, such as 07Kh16N6, opens new prospects for their application in the construction industry, where durability and structural reliability are paramount. The unique combination of mechanical strength (derived from martensitic hardening during plastic deformation) and enhanced corrosion resistance enables the development of critical structural components designed to operate under aggressive atmospheric environments and substantial mechanical loads. Specifically, the use of these steels in framework structures, fastening elements, façade systems, and engineering utilities contributes to the prolonged service life of buildings and infrastructures by mitigating corrosion-induced degradation and preventing crack formation associated with strain hardening and phase transformations.

Conclusions

Based on the conducted investigations, the following conclusions can be drawn:

(1) Crack initiation predominantly occurs along deformation-induced martensite due to the material's volume reduction during transformation, which generates tensile residual stresses. The increase in strength properties combined with a decrease in ductility of the emerging ε-martensite further exacerbates this phenomenon;

(2) After crack initiation, its propagation is not confined solely to deformation-induced martensite but can also extend into athermal martensite. Austenite that has not yet transformed at the moment of crack propagation may temporarily impede crack growth and alter its path to some extent. However, this retained austenite also undergoes transformation (primarily athermal) and crack propagation continues;

(3) To prevent crack formation, it is recommended to perform cold drawing with a maximum deformation degree not exceeding 15 %, while maintaining the deformation rate at the highest possible level;

(4) For cases requiring significant deformation (greater than 15 %), the deformation process should be carried out in multiple stages, with each deformation cycle followed by recrystallization annealing in an inert gas atmosphere at a temperature of 1050–1100 °C. Subsequent rapid cooling of the workpiece is desirable to stabilize the austenitic state.

Acknowledgements

The research was carried out within the state assignment in the field of scientific activity of the Ministry of Science and Higher Education of the Russian Federation (theme FZUN-2024-0004, state assignment of the VlSU).

REFERENCES

1. Deev V. B., Prusov E. S., Vdovin K. N., Bazlova T. A., Temlyantsev M. V. Influence of Melting Unit Type on the Properties of Middle-Carbon Cast Steel. A*RPN Journal of Engineering and Applied Sciences*. 2018. Vol. 13. No. 3. pp. 998–1001.
2. Prikhod'ko O. G., Deev V. B., Prusov E. S., Kutsenko A. I. Influence of Thermophysical Characteristics of Alloy and Mold Material on Casting Solidification Rate. *Steel in Translation*. 2020. Vol. 50 (5). pp. 296–302.
3. Prikhodko O. G., Deev V. B., Kutsenko A. I., Prusov E. S. Analysis of the Solidification Process of Castings Depending on Their Configuration and Material of the Mold. *CIS Iron and Steel Review*. 2023.Vol. 25. pp. 31–38.
4. Sergeev S. N., Safarov I. M., Zhilyaev A. P., Galeev R. M., Gladkovskii S. V., Dvoinikov D. A. Effect of Deformation-Thermal Processing on the Microstructure and Mechanical Properties of Low-Carbon Structural Steel. *Physics of Metals and Metallography*. 2021. Vol. 122. pp. 621–627.
5. Xu X., Zhang P., Fang J., Wen L., Yang Y., Zhao Y., Chen L. The hot deformation behavior and processing map analysis of a high-nitrogen austenitic stainless steel. *Journal of Materials Research and Technology*. 2024 Vol. 33. pp. 1359–1365.
6. Das C. R., Ravishankar C., Albert S. K., Krishnan S. A., Moitra A., Rajkumar K. V., Bhaduri A. K. Failure analysis of cold worked

AISI 301 SS diaphragm of gas pump. *Engineering Failure Analysis*. 2018. Vol. 92. pp. 456–465.
7. Golovkin P. A., Kryukov A. V. The effect of forging on the material structure and surface quality of workpieces during finishing turning of steel 07Kh16N6-Sh. *Tekhnologiya mashinostroeniya*. 2023. No 10. pp. 32–39.
8. Il'in A. A., Krikushenko E. S., Alekseev V. V., Silina V. I., Belousov V. V. Method of heat treatment of martensitic-aging steels 08Kh15N5D2T, 06Kh14N6D2MBT and 07Kh16N6. *Metallovedenie i termicheskaja obrabotka metallov*. 2013. No 3 (693). pp. 23–26.
9. Pomorcev E. N., Galiahmetov I. G., Chigarin V. I., Gabdullina Z. R., Livshits B. M., Basarkin Yu. A., Teslenko E. P. The introduction of a technologically advanced corrosion-resistant material instead of steel 07Kh16N6 for the manufacture of impellers of centrifugal compressors. *Kompressornaya tehnika i pnevmatika*. 2013. No 5. p. 44.
10. Osminin K. A., Chumanov I. V. Influence of technological parameters of production and chemical composition of steel grades 07Kh16N6, 09Kh16N4B on their operational characteristics. Sovremennye problemy elektrometallurgii stali. *Materialy XI mezhdunarodnoy konferentsii*. 2001. pp. 131–132.
11. Antipin N. A., Gecov L. B., Gnedenkov E. V., Mozhajskaja N. V., Rybnikov A. I., Semenov A. S. Strength and crack resistance of centrifugal compressor wheels. *Gazovaya promyshlennost*. 2017. No 11 (760). pp. 120.
12. Proskurin V. V. Influence of temperature-velocity loading conditions on the complex of mechanical properties of chromium-nickel steels. Dissertation ... of Candidate of Technical Sciences. Voronezh Technical University. Kursk, 1996. 135 p.
13. Pauls V. Ju. Main structural steels for meat processing equipment. *Inzhenernye tehnologii v selskom i lesnom khozyaistve. Proceedings of Voronezh national scientific and practical confrence*. 2020. pp. 69–73.
14. Hedström P. Deformation induced martensitic transformation of metastable stainless steel AISI 301. Licentiate thesis 2005-79, Department of Applied Physics and Mechanical Engineering, Luleå University of Technology, Sweden. 90 p.
15. Bunshah R. F., Mehl R. F. Rate of propagation of martensite. *Transactions AIME*. 1953. 197. pp. 1251–1258.
16. Olson G. B., Cohen M. A mechanism for the strain-induced nucleation of martensitic transformations. *Journal of the Less Common Metals*. 1972. Vol. 28. Iss. 1. pp. 107–118. DOI: 10.1016/0022-5088(72)90173-7.
17. Angel T. Formation of Martensite in Austenitic Stainless Steels Effects of Deformation, Temperature, and Composition. *J. Iron and Steel Inst*. 1954. Vol. 177. pp. 165–174.
18. Nohara K., Ono H., Ohashi N. Composition and grain size dependence of process-induced martensitic transformation in metastable austenitic stainless steels. *Iron and Steel*. 1977. Vol. 63. No. 5. pp. 772–782. DOI: 10.2355/tetsutohagane1955.63.5_772.
19. Patel J. R., Cohen M. Criterion for the action of applied stress in the martensitic transformation. *Acta Metall*. 1953. Vol 1. Iss. 5. pp. 531–538. DOI: 10.1016/0001-6160(53)90083-2.
20. Peckner D., Bernstein I. Handbook of stainless steels: New York (N.Y.). McGraw-Hill, 1977. 800 p.
21. Peterson S. F., Mataya M. C., Matlock D. K. The formability of austenitic stainless steels. *JOM*. 1997. 49. p. 54–58. DOI: 10.1007/BF02914352.
22. Mukarati T. W., Mostert R. J. and Siyasiya C. W. Development of a mathematical equation describing the strain hardening behaviour of metastable AISI 301 austenitic stainless steel. *IOP Conference Series: Materials Science and Engineering. Conference of the South African Advanced Materials Initiative (CoSAAMI 2019) 22–25 October 2019*. 2019. Vol. 65. No. 1. 012008. DOI: 10.1088/1757-899X/655/1/012008.
23. Montepagano D., Citi I., Guerra R., Di Nunzio P. E., Ruffini F. Enhancement of ductility of work hardened strips in AISI 301 austenitic stainless steel. *La Metallurgia Italiana*. 2022. July-August. pp. 7–15.
24. ASM HandBook Vol. 9. Metallography and Microstructures. 2004. *ASM International*. 4753 p. DOI: 10.31399/asm.hb.v09.9781627081771.
25. ASM HandBook Vol. 4A. Steel Heat Treating Fundamentals and Processes. 2013. *ASM International*. 753 p. DOI: 10.31399/asm.hb.v04a.9781627081658.
26. Ivanov S. G., Guryev A. M., Zemlyakov S. A., Guy'ev M. A., Romanenko V. V. Features of the sample preparation methodology for the automatic analysis of the carbide phase of steel Kh12F1 after cementation in vacuum using the "Thihomet PRO" software package. *Polzunovskiy vestnik*. 2020. No. 2. pp. 165–168.
27. Guryev A. M., Haraev Yu. P. Theory and practice of obtaining cast tools. Barnaul, Izdftelstvo Altaiskogo gosudarstvennogo tekhnicheskogo universiteta, 2005. 220 p.
28. Ivanov S. G., Guryev A. M., Zemlyakov S. A., Guryev M. A. The method of sample preparation of high-alloy steel samples for automatic analysis of the carbide phase. *Polzunovskiy vestnik*. 2020. No. 3. pp. 102–105.
29. Vazquez-Fernandez N. I., Soares G. C., Smith J. L. et al. Adiabatic Heating of Austenitic Stainless Steels at Different Strain Rates. *J. dynamic behavior mater*. 2019. 5. pp. 221–229. DOI: 10.1007/s40870-019-00204-z.
30. Papula S., Saukkonen T., Talonen J., Hänninen H. Delayed Cracking of Metastable Austenitic Stainless Steels after Deep Drawing. *ISIJ International*. 2015. Vol. 55. Iss. 10. pp. 2182–2188. DOI: 10.2355/isijinternational.ISIJINT-2015-078.
31. Gansel R., Heinrich C., Lohrengel A. et al. Development of Material Sensors Made of Metastable Austenitic Stainless Steel for Load Monitoring. *J. of Mater. Eng. and Perform*. 2024. Vol. 33. pp. 13570–13582. DOI: 10.1007/s11665-024-09910-9.
32. Papula S., Talonen J., Hänninen H. Effect of Residual Stress and Strain-Induced α′-Martensite on Delayed Cracking of Metastable Austenitic Stainless Steels. *Metall Mater. Trans. A*. 2014. Vol. 45. pp. 1238–1246. DOI: 10.1007/s11661-013-2090-3.
33. Li J., Li Y., Wang J., Han P. Effect of Silicon on the Martensitic Nucleation and Transformation of 301 Stainless Steel under Various Cold-Rolling Deformations. *Metals*. 2024. Vol. 14. 827. DOI: 10.3390/met14070827.
34. Hedström P., Almer J., Lienert U., Odén M. Evolution of Residual Strains in Metastable Austenitic Stainless Steels and the Accompanying Strain Induced Martensitic Transformation. *MSF*. 2006. DOI: 10.4028/www.scientific.net/msf.524-525.821.
35. Santos J. L., Monteiro S. N., Cândido V. S., da Silva A. O., Tommasini F. J., Fracture Modes of AISI Type 302 Stainless Steel Under Metastable Plastic Deformation. *Materials Research*. 2017. Vol. 20 (Suppl. No. 2). pp. 596–602. DOI: 10.1590/1980-5373-MR-2017-0051.
36. Forsstrom A., Talonen J., Saukkonen T., Hanninen H. Grain boundary engineering of metastable 204Cu, 301, and 301LN austenitic stainless steels to improve their sensitization resistance. *Materials and Corrosion*. 2015. Vol. 66. No. 2. DOI: 10.1002/maco.201407694.
37. Tiamiyu A. A., Zhao S., Li Z. et al. Thermal and Mechanical Stability of Austenite in Metastable Austenitic Stainless Steel. *Metall Mater. Trans. A*. 2019. Vol. 50. pp. 4513–4530. DOI: 10.1007/s11661-019-05362-2.
38. Leso T. P., Mukarati T. W., Mostert R., Siyasiya C. W. Strain-Induced Martensitic Transformation and the Mechanism of Wear and Rolling Contact Fatigue of AISI 301LN Metastable Austenitic Stainless Steel. *Steel Research International*. 2024. Vol. 95. No. 9. DOI: 10.1002/srin.202400128.